THE UNIVERSITY of EDINBURGH

Edinburgh Research Explorer

Role of host cell traversal by the malaria sporozoite during liver infection

Citation for published version:
Tavares, J, Formaglio, P, Thiberge, S, Mordelet, E, Van Rooijen, N, Medvinsky, A, Ménard, R & Amino, R 2013, 'Role of host cell traversal by the malaria sporozoite during liver infection', *Journal of Experimental Medicine*, vol. 210, no. 5, pp. 905-915. https://doi.org/10.1084/jem.20121130

Digital Object Identifier (DOI):
10.1084/jem.20121130

Link:
Link to publication record in Edinburgh Research Explorer

Document Version:
Publisher's PDF, also known as Version of record

Published In:
Journal of Experimental Medicine

General rights
Copyright for the publications made accessible via the Edinburgh Research Explorer is retained by the author(s) and / or other copyright owners and it is a condition of accessing these publications that users recognise and abide by the legal requirements associated with these rights.

Take down policy
The University of Edinburgh has made every reasonable effort to ensure that Edinburgh Research Explorer content complies with UK legislation. If you believe that the public display of this file breaches copyright please contact openaccess@ed.ac.uk providing details, and we will remove access to the work immediately and investigate your claim.

Download date: 27. Jul. 2024

Role of host cell traversal by the malaria sporozoite during liver infection

Joana Tavares,[1,2] Pauline Formaglio,[1] Sabine Thiberge,[1] Elodie Mordelet,[3] Nico Van Rooijen,[4] Alexander Medvinsky,[5] Robert Ménard,[1] and Rogerio Amino[1]

[1]Unité de Biologie et Génétique du Paludisme, Institut Pasteur, F-75015 Paris, France
[2]Parasite Disease Group, IBMC- Instituto de Biologia Molecular e Celular, Universidade do Porto, 4150-180 Porto, Portugal
[3]Unité Macrophages et Développement de l'Immunité, CNRS-URA 2578, Institut Pasteur, F-75015 Paris, France
[4]Department of Molecular and Cell Biology, VUMC, 1081BT Amsterdam, Netherlands
[5]Ontogeny of Haematopoietic Stem Cells Group, Institute for Stem Cell Research, University of Edinburgh, EH16 4UU Edinburgh, UK

Malaria infection starts when the sporozoite stage of the *Plasmodium* parasite is injected into the skin by a mosquito. Sporozoites are known to traverse host cells before finally invading a hepatocyte and multiplying into erythrocyte-infecting forms, but how sporozoites reach hepatocytes in the liver and the role of host cell traversal (CT) remain unclear. We report the first quantitative imaging study of sporozoite liver infection in rodents. We show that sporozoites can cross the liver sinusoidal barrier by multiple mechanisms, targeting Kupffer cells (KC) or endothelial cells and associated or not with the parasite CT activity. We also show that the primary role of CT is to inhibit sporozoite clearance by KC during locomotion inside the sinusoid lumen, before crossing the barrier. By being involved in multiple steps of the sporozoite journey from the skin to the final hepatocyte, the parasite proteins mediating host CT emerge as ideal antibody targets for vaccination against the parasite.

CORRESPONDENCE
Robert Ménard:
rmenard@pasteur.fr
OR
Rogerio Amino:
roti@pasteur.fr

Abbreviations used: CT, cell traversal; EC, endothelial cell; HGF, hepatocyte growth factor; KC, Kupffer cell; PI, propidium iodide.

The malaria-causing *Plasmodium* parasite is transmitted during the bite of an infected anopheline mosquito. The parasite, a highly motile cell called sporozoite at this stage, is inoculated into the skin of the host (Vanderberg and Frevert, 2004; Amino et al., 2006), invades dermal blood vessels to reach the bloodstream, and arrests in the liver. The sporozoite then invades a hepatocyte inside a vacuole (Meis et al., 1983a), where a single sporozoite transforms into thousands of the erythrocyte-infecting merozoite forms of the parasite (Sturm, et al., 2006). Merozoites released into the blood then invade erythrocytes, initiating the symptomatic phase of the disease of iterative parasite multiplication cycles in erythrocytes.

How sporozoites cross the liver sinusoidal barrier to reach hepatocytes has been extensively investigated, mostly using the rodent-infecting *Plasmodium berghei* species. Liver sinusoids are lined by fenestrated endothelial cells (ECs) and harbor Kupffer cells (KCs), the resident macrophages in the liver. Although KCs mainly double line the sinusoidal wall and reside inside the sinusoid lumen, they can also partly insert between ECs and directly connect the sinusoid lumen and the hepatic parenchyma (Wisse, 1974; Motta, 1984). Much of earlier (Sinden and Smith, 1982; Meis et al., 1983b; Vreden, 1994) and more recent (Pradel and Frevert, 2001; Frevert et al., 2005; Baer et al., 2007) work favors the hypothesis that sporozoites cross the sinusoidal barrier exclusively via KCs, known as the gateway model (Frevert et al., 2006). A single intravital imaging study of *Plasmodium* sporozoites in the liver was performed so far, which appeared to confirm the gateway model (Frevert et al., 2005), although the wide-field microscopy used in that study could not provide sufficient resolution to demonstrate a necessary role of KCs in sporozoite crossing (Frevert et al., 2006). The original gateway model postulated that sporozoites actively invaded KCs inside a nonfusogenic parasitophorous vacuole and transcytosed into the parenchyma (Meis et al., 1983b; Pradel and Frevert, 2001).

Elodie Mordelet's present address is INSERM U1049, Université de Bordeaux 2, 33076 Bordeaux, France.

© 2013 Tavares et al. This article is distributed under the terms of an Attribution–Noncommercial–Share Alike–No Mirror Sites license for the first six months after the publication date (see http://www.rupress.org/terms). After six months it is available under a Creative Commons License (Attribution–Noncommercial–Share Alike 3.0 Unported license, as described at http://creativecommons.org/licenses/by-nc-sa/3.0/).

The Rockefeller University Press $30.00
J. Exp. Med. 2013 Vol. 210 No. 5 905-915
www.jem.org/cgi/doi/10.1084/jem.20121130

The Journal of Experimental Medicine

Downloaded from https://rupress.org/jem/article-pdf/210/5/905/639297/jem_20121130.pdf by guest on 28 May 2020

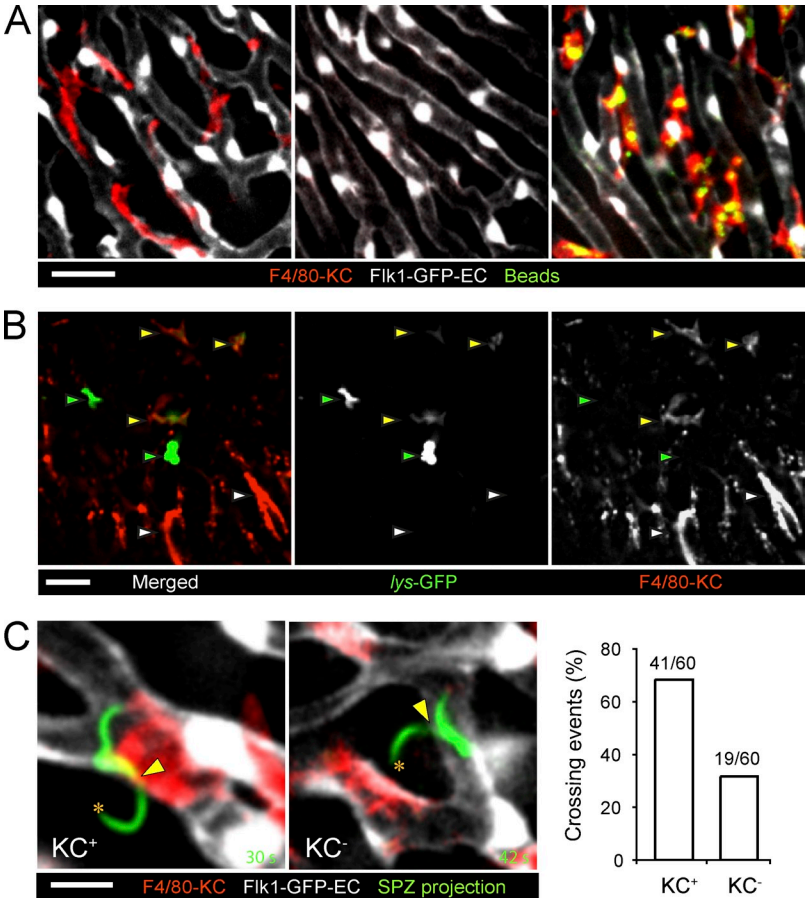

Figure 1. Crossing of the liver sinusoidal barrier by *Plasmodium* sporozoites. (A) Intravital imaging of the sinusoidal barrier in an *flk1-gfp* mouse injected intravenously with Alexa Fluor 647 anti-F4/80 antibody. GFP-expressing ECs and F4/80-labeled KCs are pseudo-colored in white and red, respectively (left). KC labeling specificity was confirmed by clodronate-depletion of phagocytic cells (middle) and by colocalization of phagocytosed fluorescent microspheres (beads in green) with F4/80 labeling (right). Images are maximal Z-projections of five contiguous pictures separated by 5 µm. Bar, 20 µm. (B) KC detection in *lys-egfp* mice. Intravital imaging of the liver of *lys-egfp* mouse injected intravenously with Alexa Fluor 647 anti-F4/80 antibody. Neutrophils (green arrowheads) and KCs (yellow arrowheads) are identified by GFP^{high} and GFP^{low} fluorescence intensities, respectively. F4/80-positive cells (pseudo-colored in red) expressing no detectable GFP are indicated by white arrowheads. Images are maximal Z-projections of three contiguous pictures separated by 5 µm. Bar, 20 µm. (C) Intravital imaging of KC-sporozoite association during sporozoite crossing. The pictures show the trajectories of RFP^+ sporozoites leaving the sinusoidal lumen and invading the hepatic parenchyma (SPZ projection in green) and are representative of the behavior scored as crossing events. KC^+ indicates the presence of a KC matching, or adjacent to, the crossing site (yellow arrowhead, left panel). KC^- indicates the absence of a KC at the invasion site (yellow arrowhead, right). The images are maximal Z-projections of three contiguous pictures separated by 5 µm and T-projected for 30 and 42 s, respectively. Asterisks indicate the final position of the parasite in the parenchyma. Bar, 10 µm. The graph shows the quantification of the KC^+ and KC^- crossing events (60 individual crossing events obtained from 25 independent experiments).

Plasmodium sporozoites can traverse host cells, i.e., breach the cell plasma membrane, glide through the cytosol, and exit the host cell (Mota et al., 2001). This cell traversal (CT) behavior was first observed with peritoneal macrophages (Vanderberg et al., 1990) and later with various other cell types, including hepatocytes (Mota et al., 2001; Amino et al., 2008). Work on sporozoite CT, also using *P. berghei*, has focused on sporozoite–hepatocyte interactions and has reported several roles of hepatocyte traversal. Hepatocyte traversal was found to render sporozoites competent for the final invasion event (Mota et al., 2002) and to facilitate parasite intravacuolar development via the activity of hepatocyte growth factor (HGF) released from traversed hepatocytes (Carrolo et al., 2003). Conversely, traversal of hepatocytes was also reported to limit the development of intracellular parasites by the expression of inducible NO synthase via MyD88-mediated NF-κB activation (Torgler et al., 2008). These hypotheses, however, are questioned by the phenotype of sporozoite mutants deficient in CT bearing null mutations in *SPECT* and *SPECT2*, which retain normal capacity to invade and develop inside hepatocytes in vitro (Ishino et al., 2004, 2005). In vivo, these mutant sporozoites were found to be poorly infective but to recover normal infectivity after KC depletion (Ishino et al., 2004, 2005). This appeared to strengthen the gateway model, suggesting that sporozoites crossed the sinusoidal barrier by KC traversal (Yuda and Ishino, 2004). Here, we investigate both the way sporozoites cross the sinusoidal barrier and the role of its CT capacity in the liver by intravital imaging of wild-type and CT-deficient sporozoites in rodents.

RESULTS

KCs are not mandatory for sporozoite crossing the liver sinusoidal barrier

To investigate the interactions of *Plasmodium* sporozoites with KCs and ECs in the liver sinusoids, the three cell types were differentially labeled and their dynamic interplay was examined in the liver of mice using intravital laser spinning-disk confocal microscopy. We used *P. berghei* sporozoites constitutively expressing RedStar fluorescent protein (RFP^+; Sturm et al., 2009). ECs were visualized using *flk1-gfp* transgenic C57BL/6 mice (Xu et al., 2010), which express GFP in ECs including in the liver sinusoids. The fluorescence of the thin EC cytoplasmic processes sharply delineated the sinusoidal lumen, thus permitting us to define the exact sites and moments of sporozoite crossing (Fig. 1). KCs were labeled using Alexa Fluor 647–conjugated anti-F4/80 monoclonal antibody injected intravenously in the

Downloaded from https://rupress.org/jem/article-pdf/210/5/905/639297/jem_20121130.pdf by guest on 28 May 2020

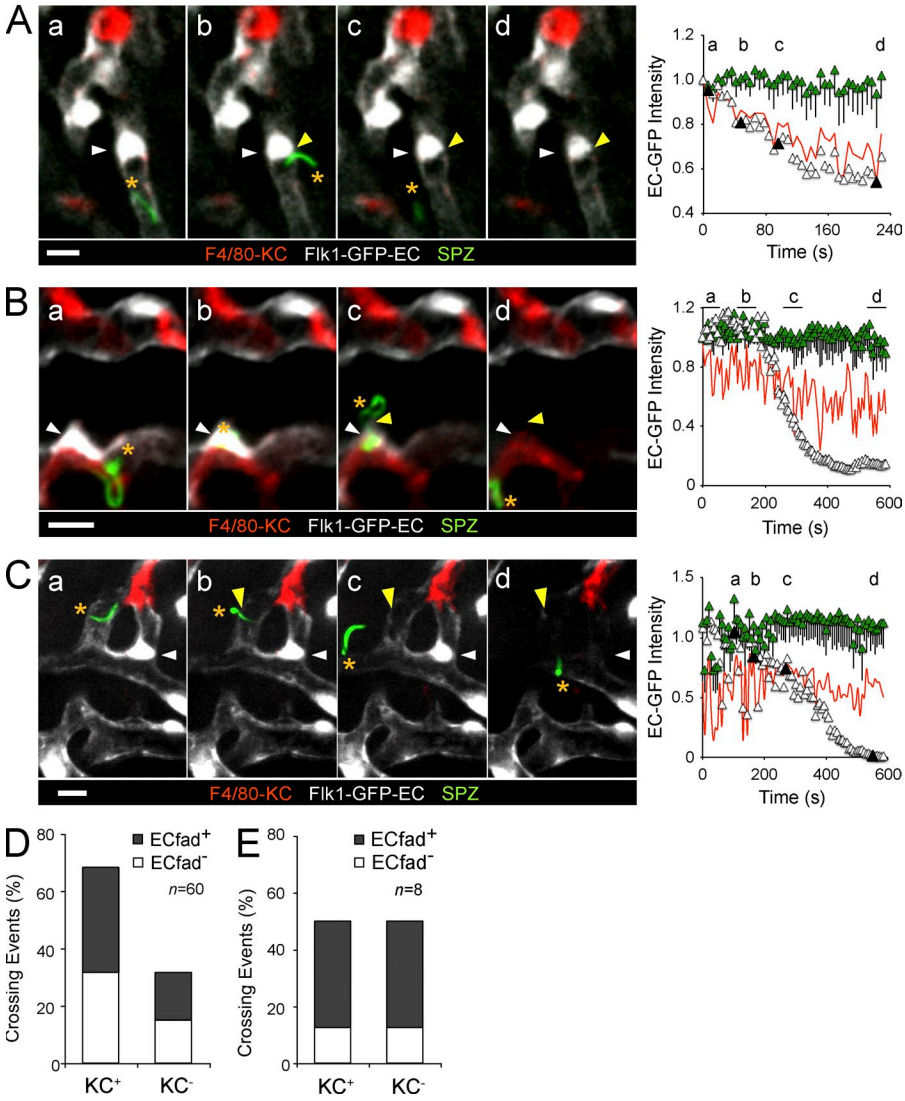

Figure 2. Crossing the liver sinusoidal barrier by EC traversal. (A–C) Time-lapse intravital confocal microscopy of RFP+ sporozoites (green) crossing the liver sinusoidal barrier through (white) ECs (yellow arrowhead) in *flk1-gfp* mice harboring (red) F4/80-labeled KCs. The white arrowheads indicate the decrease of EC-GFP fluorescence after sporozoite crossing. Images (left) are Z-projections of three contiguous pictures separated by 5 µm. Asterisks indicate the anterior poles of sporozoites. Bars, 10 µm. Graphs (right) show the quantification of normalized GFP mean intensity of ECs at the crossing site (white triangles) and in at least seven ECs from the same field and focal plane that did not interact with the parasite (green triangles, mean ± SD). The red lines represent the lower tolerance limit for 95% of the population. Dark triangles, black bars, and letters (a–d) represent the respective time-lapse images. (D and E) Quantification of crossing events by sporozoites injected via intravenous injection (D) or mosquito bite (E), classified by KC association and EC fading phenotypes. Sporozoites were delivered by intravenous injection (A, B, and D; $n = 60$ events from the same 25 independent experiments analyzed in Fig. 1 C) or mosquito bite (C and E; $n = 8$ from 15 independent experiments).

flk1-gfp mouse 30 min before sporozoite injection (Fig. 1 A, left). The F4/80 specificity was confirmed in vivo by depleting KCs with clodronate (Van Rooijen and Sanders, 1994), which completely abolished KC staining in the sinusoids (Fig. 1 A, middle). F4/80 labeling also colocalized with fluorescent beads taken up by phagocytic cells (Fig. 1 A, right) and with weakly GFP+ myelomonocytic cells in the liver of *lys-gfp* transgenic mice (Fig. 1 B). Importantly, neither the anti-F4/80 antibody nor GFP expression in ECs impaired *P. berghei* sporozoite infectivity (not depicted), and thus presumably did not alter sporozoite, EC, or KC behaviors in vivo.

After intravenous injection of ~3×10^5 RFP+ sporozoites in F4/80-labeled *flk1-gfp* mice, individual sporozoites were imaged in the left liver lobe in a volume of $125 \times 125 \times 40$ µm^3 (8–10 confocal Z-stacks) until a crossing event was observed, i.e., a sporozoite (pseudo-colored in green) translocating from the sinusoidal lumen delineated by the GFP fluorescence (pseudo-colored in white) into the black parenchyma (Fig. 1 C). 60 such crossing events were recorded, of which 68% (41/60) occurred at sites overlapping or closely adjacent to a F4/80-positive area, noted as KC+ events. At least ~32% (19/60) of the sporozoite crossing events occurred in F4/80-negative areas, i.e., without interaction with KCs at the crossing site, KC− (Fig. 1 C). We also observed that sporozoites of *P. yoelii*, another rodent-infective *Plasmodium* species, were able to cross the sinusoidal barrier in a zone lacking KCs (unpublished data). This indicated that *Plasmodium* sporozoites might cross the barrier not only through KCs but also through ECs.

Sporozoite crossing by EC traversal

When we analyzed the GFP+ ECs matching the site of sporozoite crossing during events in the KC− group, we frequently observed a rapid, specific, and significant decrease in fluorescence intensity, a phenotype we called EC fading (ECfad+), which occurred during or just before the complete passage of the sporozoite through the EC (Fig. 2 A). To determine whether the ECfad+ phenotype resulted from sporozoite traversal of ECs, we characterized the phenotype in vitro using

Downloaded from https://rupress.org/jem/article-pdf/210/5/905/639297/jem_20121130.pdf by guest on 28 May 2020

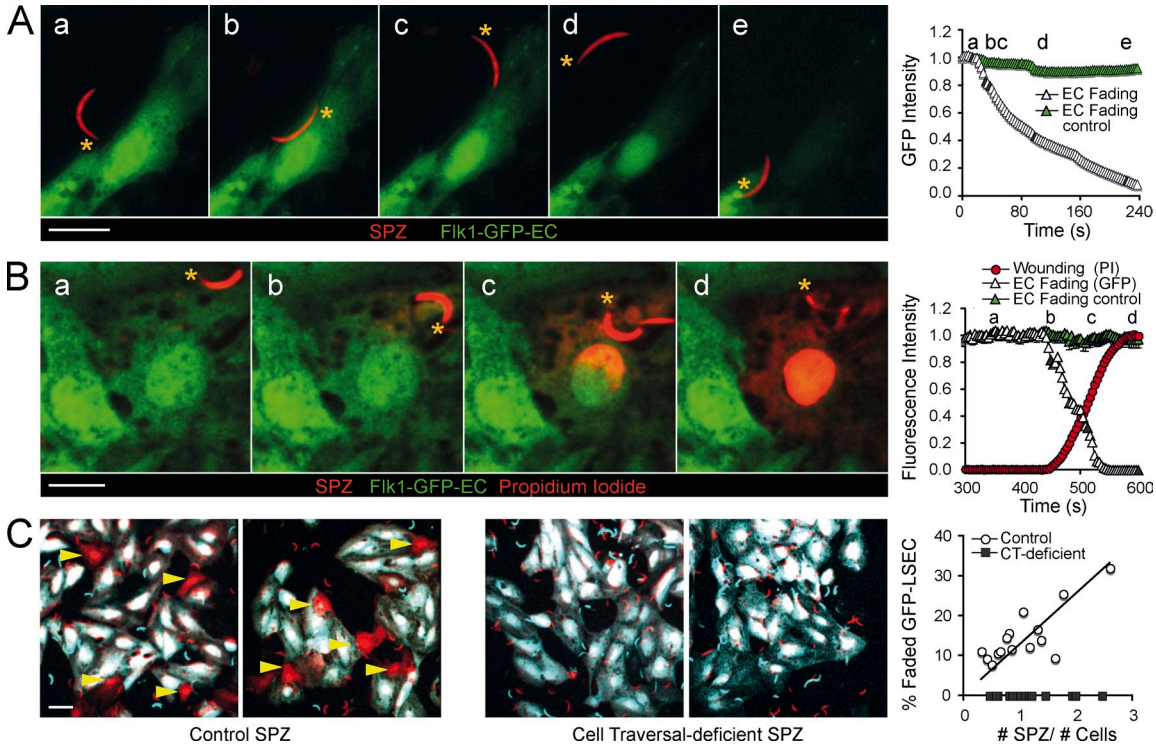

Figure 3. Fading of GFP⁺ ECs is a result of sporozoite CT activity. (A) Time-lapse microscopy of a sporozoite (SPZ, red) traversing and triggering the specific decrease of the fluorescence intensity of a primary liver sinusoidal EC (green) isolated from an *flk1-gfp* mouse. The graph quantifies EC fading based on the normalized GFP mean intensity of the traversed EC (white triangles). The EC fading control (green triangles) corresponds to adjacent ECs in the same microscopic field. Pictures are representative of 10 independent experiments. Bar, 10 µm. (B) Time-lapse microscopy of a sporozoite (red) traversing a primary GFP⁺ EC (green) in the presence of PI. The fading of the GFP⁺ EC is simultaneous to the nuclear incorporation of PI in the traversed EC (red), as observed in the images and quantified in the graph. In the graph, red circles and white triangles represent the normalized PI and GFP mean fluorescence intensities of the traversed EC, respectively. The fading control is represented by green triangles. Bar, 10 µm. In A and B, dark triangles and letters (a–d) represent the projected time-lapse images in the graph. Asterisks indicate the anterior pole of sporozoites. Pictures are representative of five independent experiments. (C) Primary GFP⁺ ECs were incubated with control sporozoites (GFP⁺ control, white circles) or CT-deficient sporozoites (GFP⁺ SPECT2⁻, black squares) and imaged dynamically by wide-field fluorescence microscopy. After 90 min of interaction, the percentage of faded GFP⁺ ECs (yellow arrowhead, red cells) was quantified and plotted according to the ratio of sporozoite per cell in the microscopic field. Pictures are representative of five independent experiments. Bar, 20 µm.

primary liver sinusoid *flk1-gfp* (GFP⁺) ECs and RFP⁺ sporozoites by dynamic microscopy. When a primary liver sinusoidal EC monolayer was incubated with sporozoites, a specific fading of EC fluorescence was frequently observed, triggered by sporozoite contact with, and presumably traversal of, ECs (Fig. 3 A), similar to the ECfad⁺ phenotype observed in vivo. To test whether the ECfad⁺ phenotype correlated with a loss of host cell membrane integrity and GFP leakage, we imaged the interactions in the presence of propidium iodide (PI), a membrane-impermeant molecule that only highly fluoresces after entry into cells and binding to nucleic acids. As shown in Fig. 3 B, the EC fading induced by sporozoites was concomitant with the increase in PI fluorescence in the EC nucleus. This suggested that sporozoites were breaching the EC plasma membrane, allowing the simultaneous entry of PI into, and leakage of GFP from, traversed ECs. To further confirm this, the EC monolayer was incubated with CT-deficient GFP⁺ SPECT2⁻ sporozoites (Amino et al., 2008) or control GFP⁺ sporozoites (Ishino et al., 2006), and sporozoite–EC interactions were imaged over 90 min by dynamic microscopy. SPECT2 is a parasite protein that contains a perforin-like domain and is essential for the sporozoite CT activity (Ishino et al., 2005). Although control sporozoites caused the fading of up to 30% of ECs, with a linear and direct relationship between the frequency of faded ECs and the ratio of sporozoite to ECs (Fig. 3 C, yellow arrowheads and graph), the GFP⁺ SPECT2⁻ sporozoites were unable to induce any detectable EC fading in the same conditions (Fig. 3 C). We conclude that the ECfad⁺ phenotype is a consequence of the sporozoite membrane wounding ability and that, in vivo, the ECfad⁺ phenotype is a signature of sporozoite traversal of ECs.

Intravital imaging revealed that ∼53% of the sporozoite crossing events (32/60) were ECfad⁺, i.e., ultimately depended on EC traversal. Of these, 16.7% were ECfad⁺ KC⁻ (Fig. 2, A and D), corresponding to crossing events by direct EC traversal, whereas 36.6% were ECfad⁺ KC⁺ (Fig. 2, B and D), corresponding to crossing events by EC traversal after interactions with a KC. Finally, because prior observations were made after intravenous injection of sporozoites,

Downloaded from https://rupress.org/jem/article-pdf/210/5/905/639297/jem_20121130.pdf by guest on 28 May 2020

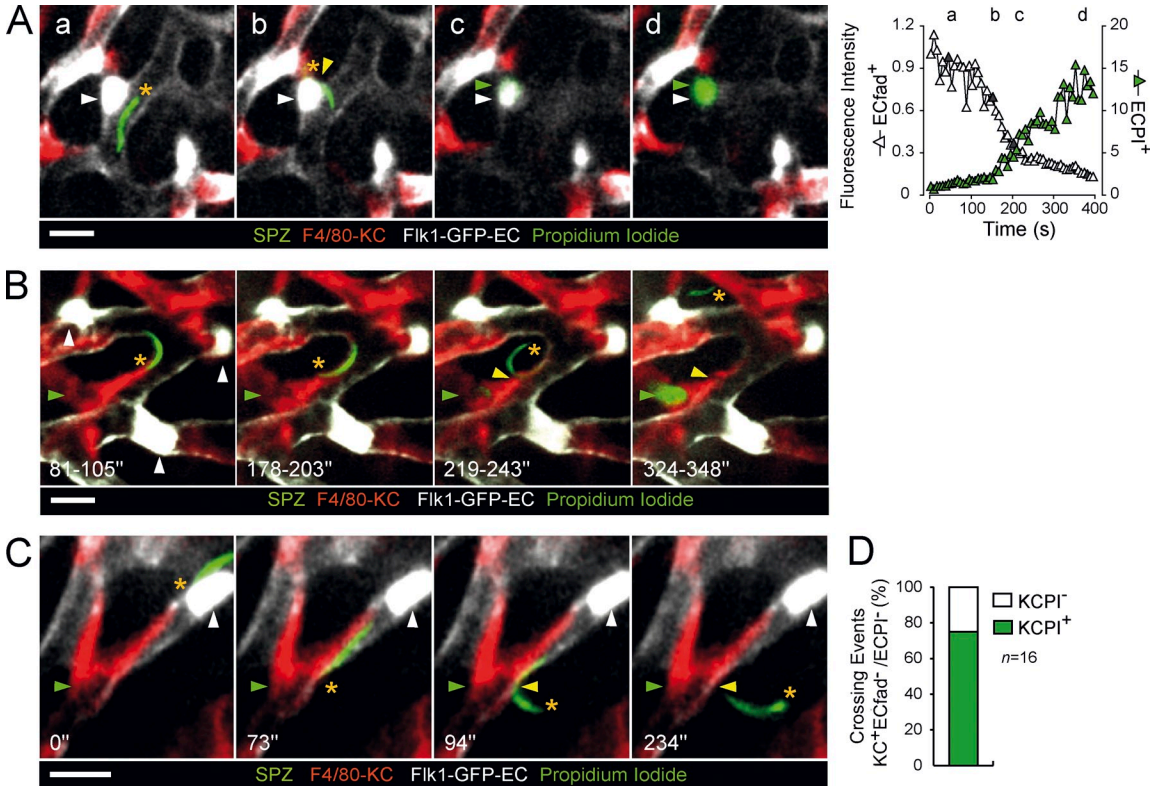

Figure 4. KC-related crossing of the liver sinusoidal barrier. (A–C) RFP+ sporozoites were intravenously injected in *flk1-gfp* mice labeled with anti-F4/80 antibody and imaged in liver sinusoids in the presence of PI in 20 independent experiments. (A) Time lapse of a sporozoite (green) crossing the barrier (yellow arrowhead) through EC traversal, with simultaneous EC fading (white arrowheads) and PI incorporation (green arrowheads, ECPI+). The graph shows the simultaneous loss of the normalized GFP+ EC fluorescence intensity and the increase of the PI fluorescence intensity in the EC nucleus. Dark triangles and letters (a–d) represent the respective time-lapse images in the graph. (B) Time lapse of a sporozoite (green) crossing the barrier through KC traversal (yellow arrowheads) visualized by the nuclear PI incorporation in the traversed KC (green arrowheads, KCPI+). (C) Time lapse of a KC+ crossing event (yellow arrowheads) without PI incorporation in the KC (green arrowheads, KCPI−). In B and C, white arrowheads indicate EC lining the site of crossing that did not fade or become PI+ during crossing. Images are maximal Z-projections of three contiguous planes separated by 5 µm. T-projections are indicated at the panel bottom (white time interval). Asterisks mark the anterior pole of sporozoites. Bars, 10 µm. (D) Quantification of the crossing events through KC traversal, represented by the phenotype KCPI+, ECfad−/ECPI− (green bar).

an inoculation route which bypasses the natural first steps of the sporozoite in the skin and might thus impact sporozoite behavior in the liver sinusoids, we also imaged sporozoites after inoculation by mosquito bites. Although only few crossing events (n = 8) could be recorded, reflecting the small number of sporozoites inoculated by natural transmission, most were associated with an ECfad+ phenotype (Fig. 2, C and E) similar to that induced by sporozoites injected intravenously. Therefore, although these data are too limited to allow an estimation of the proportion of crossing events by EC traversal after sporozoite inoculation in the skin, they show that the ECfad+ phenotype is not an artifact of the intravenous inoculation route. Sporozoites, including those inoculated in the skin, can use CT to cross the liver sinusoidal barrier via EC traversal.

Sporozoite crossing by KC traversal

We next focused on the crossing events that involved KCs (KC+) but did not depend on EC traversal (ECfad−), which represented 32% of the total crossing events observed. To monitor KCs during such ECfad− KC+ crossing events, we established a PI wounding assay (Tavares et al., 2013) for in vivo detection of KC wounding. We first validated the use of PI as a marker of cell wounding in vivo using ECs as target cells. PI was injected subcutaneously in an *flk1-gfp* mouse, RFP+ sporozoites and anti-F4/80 antibody were injected intravenously, and the proportions of crossing events causing the ECfad+ phenotype and the incorporation of PI in the EC nucleus, called ECPI+ phenotype, were compared. As exemplified in Fig. 4 A, most ECfad+ events were also ECPI+ (16/17), which validated PI incorporation as a marker of cell wounding in vivo. We then used the PI intravital assay to quantify the proportion of ECfad− KC+ crossing events that wounded KCs and caused PI incorporation in its nucleus, noted as KCPI+ phenotype. The majority (∼75%) of the ECfad− KC+ events were associated with a KCPI+ phenotype (Fig. 4, B and D). These ECfad− KC+ KCPI+ events were also ECPI− (Fig. 4 B), confirming the absence of EC traversal. These events were thus compatible with sporozoites crossing the barrier by KC traversal.

Downloaded from https://rupress.org/jem/article-pdf/210/5/905/639297/jem_20121130.pdf by guest on 28 May 2020

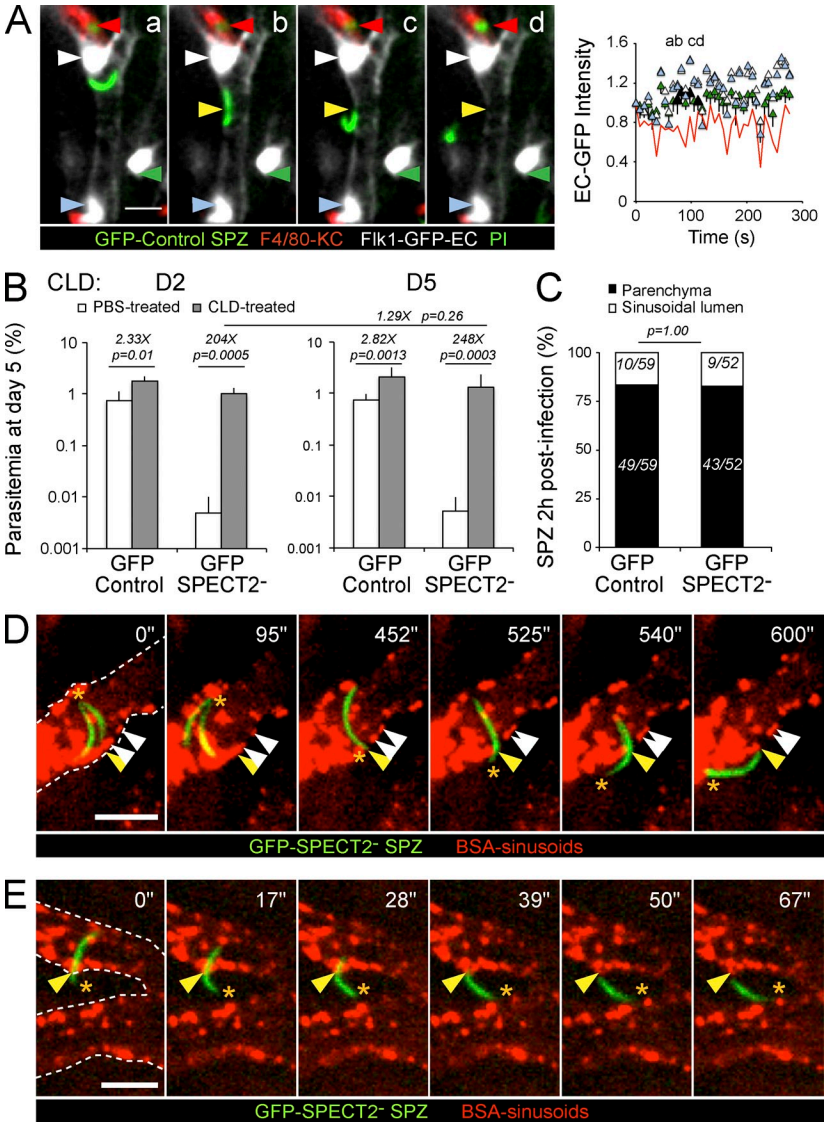

Figure 5. CT-independent crossing of the liver sinusoidal barrier. (A) Time-lapse intravital confocal microscopy of sporozoites (green) crossing the barrier via (white) ECs in a *flk1-gfp* mouse harboring (red) F4/80-labeled KCs. White and blue arrowheads show the EC$^+$ GFP fluorescence after sporozoite crossing (yellow arrowheads). Red arrowheads show a PI positive KC. Images are Z-projections of three contiguous pictures separated by 5 µm. Bar, 10 µm. The graph shows the quantification of normalized GFP mean intensity of the two ECs in the vicinity of the crossing site (white and blue triangles) and in seven ECs from the same field and focal plane that did not interact with the parasite (green triangles, mean ± SD). The red line represents the lower tolerance limit of 95% of the population. (B) SPECT2$^-$ sporozoite infectivity in C57BL/6 mice after depletion of KCs by intravenous injection of clodronate liposomes 2 or 5 d before infection. Control mice received PBS. Groups of mice (n = 4) were infected intravenously with 2 × 10^4 GFP$^+$ control or GFP$^+$ SPECT2$^-$ sporozoites and parasitemia was quantified by FACS analysis at day 5 after infection. A representative experiment from three independent experiments is shown. The bars and error bars represent the mean parasitemia and one SD, respectively. (C) Percentage of GFP$^+$ control and GFP$^+$ SPECT2$^-$ sporozoites in the liver parenchyma and sinusoidal lumen. 2 h after intravenous injection of parasites in C57BL/6 mice depleted of phagocytic cells, sporozoites were counted by intravital confocal microscopy in 30 fields of 125 × 125 × 40 µm^3 each. (D and E) Time lapses representative of CT-deficient sporozoites (green, GFP$^+$ SPECT2$^-$) crossing the liver sinusoidal barrier (red, Alexa Fluor 555-BSA) of C57BL/6 mice in which phagocytic cells were depleted by clodronate treatment. Images are maximal Z-projections of three contiguous planes separated by 5 µm. Asterisks indicate the anterior pole of sporozoites and yellow and white arrowheads indicate the sporozoite crossing site and the dynamics of BSA$^+$ endocytic vesicles, respectively. The area delineated by dotted lines is the lumen of the sinusoid. Bars, 10 µm.

CT-independent sporozoite crossing

The remainder (~25%) of the ECfad$^-$ KC$^+$ events, representing ~8% of the total crossing events, did not cause PI incorporation in the contacted KC, KCPI$^-$ (Fig. 4, C and D), or in ECs (ECPI$^-$). These crossing events are compatible with the invasion-transcytosis variant of the gateway model but could also correspond to parasites crossing the barrier between adjacent KCs and ECs.

Finally, ~15% of the total crossing events were associated with an ECfad$^-$ KC$^-$ phenotype (Fig. 5 A), indicating sporozoites crossing at a distance of KC without traversing an EC. This phenotype is compatible with a paracellular pathway, i.e., between two ECs, or with a transcellular pathway, i.e., through ECs but without loss of membrane integrity. The existence of CT-independent crossing paths is in agreement with the findings that CT-deficient sporozoites, e.g., SPECT$^-$, SPECT2$^-$, and CelTOS$^-$, which are all defective in CT activity (Ishino et al., 2004; 2005; Kariu et al., 2006), can all induce a blood infection, albeit with reduced efficiency. To further investigate CT-independent crossing, we imaged GFP$^+$ SPECT2$^-$ sporozoites in KC-depleted mice, in which SPECT2$^-$ sporozoites recover normal infectivity after intravenous injection (Ishino et al., 2005; Fig. 5 B). GFP$^+$ SPECT2$^-$ or GFP$^+$ control sporozoites were injected intravenously into mice and the numbers of sporozoites present in the liver parenchyma 2 h after injection were compared by intravital imaging (Fig. 5 C). Similar numbers of control and SPECT2$^-$ sporozoites had reached the parenchyma 2 h after injection, confirming that the CT activity is not essential for sporozoite crossing the sinusoidal barrier and that CT-independent crossing mechanisms are operational in sporozoites. We also imaged crossing events by GFP$^+$ SPECT2$^-$ sporozoites in KC-depleted (Fig. 5, D and E) as well as KC-harboring (*lys-gfp*, not depicted) mice, which revealed sporozoites translocating

Downloaded from https://rupress.org/jem/article-pdf/210/5/905/639297/jem_20121130.pdf by guest on 28 May 2020

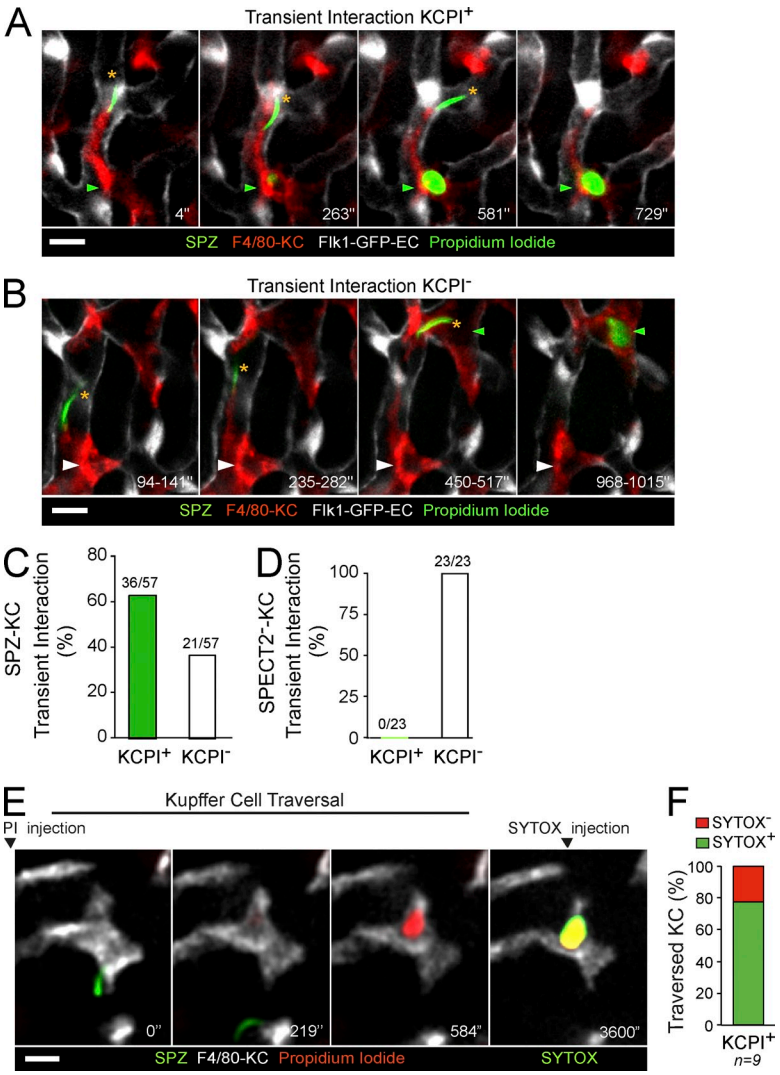

Figure 6. Sporozoites gliding in the sinusoids wound and kill KCs. (A and B) RFP+ sporozoites (green) were intravenously injected in *flk1-gfp* mice labeled with anti-F4/80 antibody and imaged in the presence of PI 5 mg/kg (green) in the liver sinusoids by intravital confocal microscopy. Time lapses are representative of the two types of transitory interaction of sporozoites with KCs (red) in the sinusoid lumen. Images are maximal Z-projections of three contiguous planes separated by 5 µm and T-projected according to the time indicated in white (bottom right corner). Asterisks indicate the anterior pole of sporozoites. Green and white arrowheads point to the nuclei of KCs that became PI+ (KCPI+) and PI− (KCPI−) upon interaction with sporozoites, respectively. (C and D) Quantification of the percentage of KCs that incorporate PI upon transitory interaction with control (C) or SPECT2− (D) sporozoites. (E) Fate of a traversed KC, monitored by PI incorporation (0–584 s) and after 1 h by incorporation of SYTOX-Green injected intravenously (1 µmol/kg). (F) Of the nine traversed KCs identified by PI incorporation, seven incorporated SYTOX-Green after 1 h ($n = 9$ from five independent experiments). Bars, 10 µm.

apparently through ECs characterized by the intracellular movement of endocytic vesicles containing BSA. However, in the absence of appropriate intercellular junction markers, we could not discriminate between paracellular and transcellular routes.

Sporozoites gliding in the liver sinusoids wound and kill KCs

Using the intravital PI assay, we imaged F4/80-labeled KCs interacting with RFP+ sporozoites gliding inside sinusoids of *flk1-gfp* mice. First, we evaluated the percentage of KC wounding, indicated by the appearance of a KCPI+ phenotype after a transient interaction with a gliding sporozoite. Transient interactions were defined by the superposition of KCs and sporozoite fluorescent signals or by KC extensions surrounding the parasite for at least 2 min (Fig. 6, A and B). The majority (~60%) of such short-lived interactions caused a KCPI+ phenotype (Fig. 6, A and C). The 40% of KCs that remained PI− were indeed not wounded rather than not stained as a result of low PI concentration because other cells were frequently observed becoming PI+ in the same microscopic field (Fig. 6 B). When CT-deficient GFP+ SPECT2− sporozoites were imaged in the same conditions, PI incorporation into the nuclei of interacting KCs was not observed (Fig. 6 D). This showed that while gliding in the sinusoids, and irrespective of barrier crossing, sporozoites transiently interact with, and frequently wound KCs.

We then evaluated the fate of KCs traversed by sporozoites using a double wounding assay. To detect KC traversal, we injected GFP+ sporozoites and PI in F4/80-labeled C57BL/6 mice and scored sporozoite–KC interactions that resulted in the KCPI+ phenotype. After 1 h, we injected SYTOX green and assessed its incorporation in the nuclei of traversed KCs (KCPI+, Fig. 6 E). SYTOX is a fluorescent dye frequently used to detect dead cells; it does not penetrate live cells and its fluorescence increases upon nucleic acid binding. Of the nine traversed KCs identified by PI incorporation, seven incorporated SYTOX after 1 h (Fig. 6 F). This suggests that most KC traversal events permanently alter KC plasma membrane integrity and presumably kill traversed KCs.

Downloaded from https://rupress.org/jem/article-pdf/210/5/905/639297/jem_20121130.pdf by guest on 28 May 2020

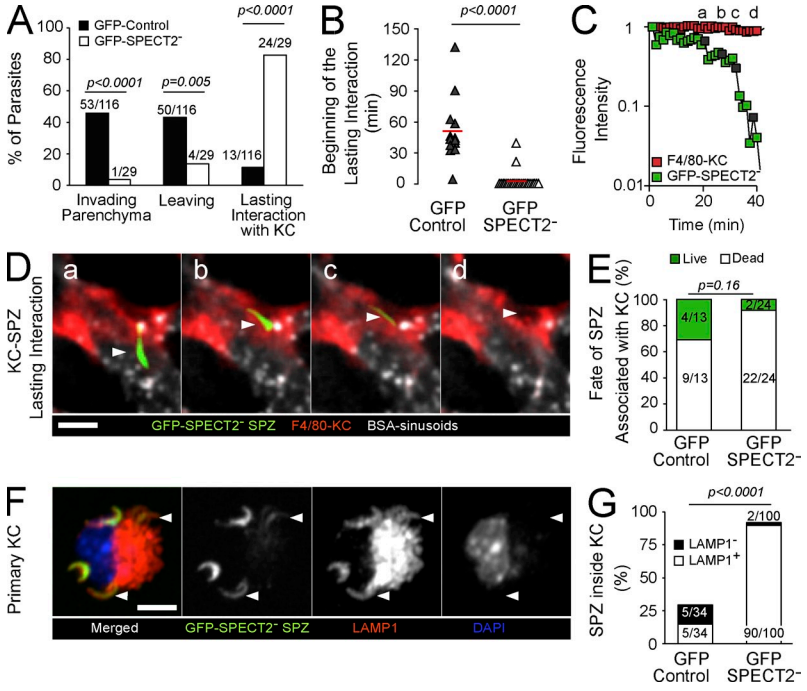

Figure 7. CT prevents sporozoite clearance by KCs in the liver sinusoids. (A) Percentage of sporozoites (GFP+ control, black symbols; GFP+ SPECT2−, white symbols) lying in the parenchyma (invading parenchyma) or associated with KCs (lasting interaction with KC) after 150 min of recording, and of sporozoites that left the field during the recording (leaving). P-values were determined by Fischer's exact test. (B) Graph indicating when sporozoites started the lasting interaction with KC (red bars, mean). P-values were determined by Wilcoxon rank-sum test. (C) Graph quantifying the fluorescence intensity of GFP+ SPECT2− sporozoites (green) or F4/80-labeled KC (red) normalized to the initial time point. Dark squares and letters (a–d) in the graph represent the respective time-lapse images from D. (D) Representative time-lapse of a KC-SPECT2− sporozoite lasting interaction leading to a gradual decrease in sporozoite fluorescence intensity (white arrowheads). Sporozoites were intravenously injected in mice labeled with anti-F4/80 antibody (KCs in red) and Alexa Fluor 555 BSA (sinusoids in white). (E) Percentage of parasites presenting a >10-fold decrease in the initial GFP intensity signal during the lasting association with KCs, scored as dead sporozoites (dead SPZ, white bars). (F and G) GFP+ control and GFP+ SPECT2− sporozoites were incubated in vitro with primary KCs for 1 h, and cells were fixed and stained with anti-CS 3D11 monoclonal antibody conjugated with Alexa Fluor 647 to discriminate between intracellular (GFP+) and extracellular (GFP+CS+) parasites. Cells were then permeabilized and stained with monoclonal antibodies to LAMP1 (clone 1D4B). (F) GFP+ SPECT2− sporozoites inside a primary KC are in LAMP1-positive compartments. White arrowheads indicate sporozoites with reduced GFP fluorescence. Images are maximal Z-projections of 10 contiguous pictures separated by 1 µm. (G) Graph showing the quantification of GFP+ control and GFP+ SPECT2− sporozoites that are inside KCs in LAMP1-positive or -negative compartments. (D and F) Bars, 10 µm.

CT prevents sporozoite clearance by KCs

The ∼2.5-fold increase in parasitemia that was reproducibly obtained after injection of sporozoites into clodronate-treated compared with untreated mice (Fig. 5 B, $P < 0.05$) suggested a negative impact of KCs on parasite infectivity. Because KCs play an important role in removing microorganisms from the blood circulation (Helmy et al., 2006), we tested whether sporozoite CT activity could play a role in resisting clearance by KCs.

For this, we analyzed the fate of CT-deficient GFP+ SPECT2− sporozoites interacting with KCs. GFP+ SPECT2− and GFP+ control sporozoites were injected intravenously into C57BL/6 mice harboring F4/80-labeled KCs and imaged in the liver for 150 min. After this time, most control sporozoites had left the microscopic field (∼48%) or invaded the parenchyma (∼45%). In contrast, only ∼14 and 3% of the GFP+ SPECT2− sporozoites had left the observation field and invaded the parenchyma, respectively (Fig. 7 A). As expected, most (∼83%) of the CT-deficient sporozoites were trapped in lasting interactions with KCs; importantly, these interactions started from the beginning of the imaging period (Fig. 7 B). In contrast, only ∼10% of control sporozoites displayed similar lasting interactions with KCs, which only started to occur ∼30 min after injection, possibly involving sporozoites that had exhausted their CT capacity (Fig. 7, A and B). For both populations of early KC interactions with SPECT2− and late KC interactions with control sporozoites, sporozoite fluorescence gradually decreased with time until undetectable levels (Fig. 7, C and D). Therefore sporozoite CT helps evading clearance by KCs.

Lastly, we compared the fate of GFP+ SPECT2− and GFP+ control sporozoites inside primary KCs in vitro. Primary KCs were purified, incubated with control or SPECT2− sporozoites for 1 h, and samples were stained using a double labeling assay to discriminate internalized and extracellular zoites (Fig. 7, E and F). More than 90% of the SPECT2− and ∼30% of control sporozoites were located inside cells ($P < 0.0001$, Fig. 7 E). Samples were also stained with antibodies to the lysosome marker LAMP1 (Fig. 7, F and G). Almost all intracellular SPECT2− sporozoites colocalized with LAMP1 staining, suggesting they were inside phagolysosomes, and frequently displayed dim green fluorescence. In contrast, only half of control, internalized sporozoites were associated with LAMP1 staining, confirming that WT sporozoites can also be phagocytosed by KCs. Presumably, the other half corresponds to traversing sporozoites or sporozoites internalized inside a parasitophorous vacuole. We conclude that sporozoite CT confers resistance to phagocytosis by KCs and likely other phagocytic cells.

DISCUSSION

This study provides the first comprehensive picture of how malaria sporozoites infect the liver and reach their final destination inside a hepatocyte. Our spinning-disk confocal imaging approach using *flk1-gfp* mouse harboring F4/80-labeled KC allowed a clear delineation of the sinusoids and a precise definition of the sporozoite crossing sites. It demonstrated that KCs do not constitute a mandatory gateway for *Plasmodium* sporozoites and revealed the multiplicity of *P. berghei* sporozoite

Downloaded from https://rupress.org/jem/article-pdf/210/5/905/639297/jem_20121130.pdf by guest on 28 May 2020

crossing mechanisms. Most crossing events (~77%, $n = 60$) were associated with CT activity. Of these, the majority occurred through ECs (53%), sometimes also involving a KC presumably double lining the traversed EC, whereas some CT events also occurred specifically through KCs (~24%). Approximately a quarter (23%) of the crossing events were CT-independent, presumably accounting for the residual capacity of CT-deficient mutants to cross normal sinusoidal barriers (Ishino et al., 2004, 2005; Kariu et al., 2006). These CT-independent crossing events might correspond to a paracellular pathway, between two ECs or between an EC and a KC, as has been suggested for *Toxoplasma* tachyzoite transmigration of cultured cell monolayers (Barragan et al., 2005). Alternatively, sporozoites could use a transcellular pathway through the formation of channels inside ECs, like those generated by extravasating leukocytes (Carman and Springer, 2004), or use and manipulate the fenestrations of liver sinusoidal ECs (Warren et al., 2007).

Another unresolved question was the role of the CT activity of the sporozoite during liver infection. Much emphasis has been put on the positive impact of hepatocyte traversal on parasite infection via the release of HGF from traversed hepatocytes, which was proposed to act on neighboring invaded cells and to facilitate parasite development (Mota and Rodriguez, 2004). Conversely, it was also proposed that WT, but not CT-deficient sporozoites, induced the expression of iNOS via activation of NF-κB, causing an approximately twofold decrease in parasite development inside hepatocytes (Torgler et al., 2008). In any event, these opposed effects in artificial in vitro conditions were minor and cannot account for the >20-fold and >100-fold reduction in the in vivo infectivity of *P. berghei* CT-deficient mutants after intravenous and subcutaneous injection, respectively (Ishino et al., 2004, 2005; Kariu et al., 2006; Amino et al., 2008). Therefore, the primary role of CT in the liver appears to be unrelated to hepatocyte traversal.

Here, we imaged a dual function of sporozoite CT in the liver. First, WT sporozoites wounded and, presumably, traversed KCs while gliding in the sinusoids, whereas the vast majority of the CT-deficient sporozoites were rapidly trapped and subsequently degraded inside KCs. This vital function of CT in avoiding parasite clearance is also likely to help the sporozoite resist attacks from other phagocytic cells than KCs, as visualized for granulocytes in *lys-gfp* mice (unpublished data). Second, CT was associated with ~80% of the crossing events through ECs and/or KCs. However, the contribution to sporozoite infectivity of CT-dependent crossing of the sinusoidal barrier is more difficult to assess. CT-deficient sporozoites reached the parenchyma as efficiently as controls in the absence of KCs, showing that CT-independent mechanisms are sufficient to allow efficient barrier crossing. Nonetheless, in the presence of KCs the availability of CT-dependent crossing mechanisms might offer an advantage by reducing the time spent in the sinusoids and decreasing the risk of clearance by phagocytic cells. We also reported previously an important role of sporozoite CT in the skin after sporozoite deposition during natural mosquito transmission, in allowing normal sporozoite progression through the dermis and access to skin vessels (Amino et al., 2008). Together, these intravital imaging data suggest a dual role of the CT activity of the sporozoite, in allowing progression through cellular barriers at multiple steps of the sporozoite journey from the skin to the liver parenchyma and escape from host cell phagocytic activity along the journey. In comparison, hepatocyte traversal appears to add little to parasite infectivity. That sporozoites first traverse several hepatocytes before invading the final one might simply result from the time necessary to repress the CT activity, which would otherwise rupture the parasitophorous vacuole membrane and prevent successful invasion.

Sporozoite CT might have additional effects, for example on adaptive immunity. Indeed sporozoites traverse hepatocytes, KCs, and ECs, which can efficiently present antigens (Ebrahimkhani et al., 2011). The shedding of parasite surface antigens in these traversed cells might induce host tolerance or immunity to the corresponding antigens, possibly presented directly by traversed cells if they recover from CT, or via other antigen-presenting cells if they die. Our data indicate that most KC wounding/traversal events result in permanent alteration of KC plasma membrane integrity, and thus likely in KC death, which might affect mounting of a protective immune response. The repeated KC traversal events during the extensive sporozoite gliding in the liver sinusoids might also liberate antiinflammatory mediators such as IL-10 and TGF-β from traversed KCs (Klotz and Frevert, 2008), which might negatively impact antiparasite immunity.

The notion that the CT activity is important to the sporozoite at many steps of its progression from the skin to the final hepatocyte makes the proteins involved in the process attractive targets for antibody-mediated inhibition strategies. High levels of antibodies against SPECT2 correlate with protection from malaria episodes caused by *P. falciparum* in children (Crompton et al., 2010). Moreover, immunization using CelTOS, another important protein involved in CT, protects rodents from challenge with sporozoites by a combination of antibody and cell-mediated effector responses (Bergmann-Leitner et al., 2011). Many parasite proteins have been described as being involved in the CT phenotype, e.g., SPECT (Ishino et al., 2004), PL (Bhanot et al., 2005), TLP (Moreira et al., 2008), and GEST (Talman et al., 2011), in addition to CelTOS (Kariu et al., 2006) and the perforin-like SPECT2 (Ishino et al., 2005). Along with antibodies to the CS protein, which inhibit sporozoite motility in the dermis (Vanderberg and Frevert, 2004) and presumably elsewhere, antibodies targeting the CT-associated factors would likely add in preventing sporozoites from reaching their final destination in the liver.

MATERIALS AND METHODS

Parasites, mice, and mosquitoes. We used *P. berghei* ANKA clones expressing the GFP under the control of the *hsp70* regulatory regions (GFP-Control; Ishino et al., 2006), the RFP under the control of *eef1-α* regulatory regions (line L733; Sturm et al., 2009), and the CT-deficient parasite SPECT2$^-$, expressing the GFP under the control of the *hsp70* regulatory regions (GFP-SPECT2$^-$; Amino et al., 2008).

C57BL/6 and Swiss mice were purchased from Elevage Janvier. *Flk1-gfp* C57BL/6 transgenic mice (Xu et al., 2010) were maintained by breeding heterozygous males with C57BL/6 females. All animal experiments were approved

Downloaded from https://rupress.org/jem/article-pdf/210/5/905/639297/jem_20121130.pdf by guest on 28 May 2020

by the Animal Care and Use committee of Institut Pasteur and were performed in accordance with European guidelines and regulations.

Anopheles stephensi mosquitoes (Sda500 strain) were reared in the Centre for Production and Infection of Anopheles (CEPIA) at the Pasteur Institute using standard procedures. Mosquitoes were fed on infected mice 1–2 d after emergence and kept as previously described (Amino et al., 2007). Infected mosquitoes used for transmission experiments (18–25 d after the infectious blood meal) were deprived of sucrose for 1 d before experimentation to enhance the rate of mosquito bite. For intravenous injections and for in vitro experiments, sporozoites were isolated from infected salivary glands 18–25 d after the infectious blood meal.

Spinning disk confocal intravital microscopy and image analysis. Mice were anesthetized with a mixture of ketamine and xylazine (ketamine: 125 mg/kg body weight; xylazine: 12.5 mg/kg body weight). Animals were prepared for intravital microscopy of the liver as described previously (Thiberge et al., 2007). In brief, once deeply anesthetized, a small left-ventral abdominal incision was made to expose the left liver lobe. The exposed lobe was moistened with a drop of phosphate buffer saline and immobilized on a coverslip with cyanoacrylate glue. The animal was placed on a motorized stage of an inverted Axiovert 200 microscope (Carl Zeiss) and covered with a heating blanket at 37°C. Images were acquired in the Imaging Platform at the Pasteur Institute (PFID) using a spinning disk confocal system (Ultraview; Perkin Elmer) composed of a Confocal Scanner Unit (CSU22; Yokogawa) with a camera (EMCCD C-9100; Hamamatsu) and 4 Diode Pumped Solid State Laser (excitation wavelengths: 405, 488, 561, and 647 nm) controlled by Volocity (Perkin Elmer). Usually continuous images were acquired using an LCI Plan-Neofluar 25×/0.8 Imm Corr DIC objective (Carl Zeiss) for up to 10 min and covering 40 µm in depth (8–10 Z-stacks). Image files were processed using ImageJ (National Institutes of Health). Liver sinusoids were visualized by the specific expression of GFP in the EC of *flk1-gfp* mice or by the intravenous injection of 50 µg Alexa Fluor 555 BSA in C57BL/6 mice. To visualize KC, 4 µg Alexa Fluor 647 anti–mouse F4/80 antibody (clone BM8; BioLegend) was intravenously injected 30 min before observation. The F4/80 labeling specificity was confirmed in vivo by depletion of phagocytic cells with clodronate liposomes (10 µl/g) injected intravenously 2 d before the antibody. Phagocytic cells in the sinusoids were detected 30 min after intravenous injection of 5 µl of a 2% suspension of red fluorescent (580/605) carboxylate-modified microspheres (0.1 µm; Molecular Probes). Sporozoites were injected either intravenously ($\sim 3 \times 10^5$) or by mosquito bite (anesthetized mice were placed on top of a mosquito cage containing 50–100 mosquitoes for 20 min). To detect host cell wounding by sporozoites mice were subcutaneously injected with PI (5 mg/kg in PBS; Invitrogen) according to Tavares et al. (2013).

Isolation of ECs and KCs from the liver. GFP$^+$ ECs were isolated from *flk1-gfp* mice according to Klugewitz et al. (2002). In brief, the livers of anesthetized mice were perfused by the portal vein with 2 ml of a 37°C prewarmed digestion medium (RPMI 1640 supplemented with 5% FBS [Cambrex], 2 mg/ml collagenase IV [Sigma-Aldrich], and 0.2 mg/ml DNase [Sigma-Aldrich]). The livers were then removed, cut in small pieces, and incubated in the digestion medium at 37°C for an additional 15 min. Cell suspension was passed through a 100 µm cell strainer and subjected to a density gradient centrifugation with 26% Optiprep (Axis Shield). GFP$^+$ ECs were further purified by magnetic cell sorting using anti-CD146 microbeads (Miltenyi Biotec). The cells were plated in a collagen I (Invitrogen)–coated 8-well µ-Slide (Ibidi) and incubated in RPMI 1640 supplemented with 10% FBS (Cambrex), 1% penicillin (Invitrogen), and 1% streptomycin (Invitrogen) at 37°C, 5% CO_2. After overnight culture, cells debris was removed and cells were used for experiments with sporozoites 2 d after isolation.

KCs were isolated from *flk1-gfp* mice according to Smedsrød and Pertoft (1985). In brief, the liver cell suspension prepared as described above was layered on a two-step Percoll gradient (bottom and overlaying cushions density of 1.066 g/ml and 1.037 g/ml, respectively) and centrifuged at 800 *g* for 15 min at 4°C. The KC-enriched fraction, extending throughout the lower Percoll cushion, was collected and washed with PBS. The cells were plated in 8-well µ-Slides (Ibidi) and incubated in RPMI 1640 supplemented with 10% FBS (Cambrex), 1% penicillin (Invitrogen), and 1% streptomycin (Invitrogen) at 37°C, 5% CO_2 for 30 min. Non-adherent cells were removed and cells were used for experiments with sporozoites the day after.

In vitro CT assay. GFP-EC traversal activity of sporozoites was visualized using the spinning-disk system equipped with a xy-automated stage. Control (GFP-Control or RFP$^+$) or CT-deficient (GFP-SPECT2$^-$) fluorescent sporozoites were incubated with primary GFP-ECs in RPMI 1640 supplemented with 10% FBS (Cambrex), 1% penicillin (Invitrogen), and 1% streptomycin (Invitrogen) at 37°C, 5% CO_2. In some experiments, the assay was performed in the presence of 10 µg/ml of PI (Invitrogen). Usually continuous images from 10–15 different fields were acquired for up to 90 min.

Statistical analysis. The lower limit of the tolerance interval containing 95% of the fluorescence values of the control population was calculated with 95% of confidence using the R software (R Core Team; http://www.R-project.org/). Values below the tolerance limit were considered statistically significant. Categorical variables were compared using two-tailed Fisher's exact test using GraphPad. Differences in the parasitemia and in the distribution of lasting interaction were analyzed using two-tailed Student's *t* test and Wilcoxon rank-sum test, respectively. P values <0.05 were considered statistically significant.

We thank S. Shorte and the Dynamic Imaging Platform (PFID-Institut Pasteur) for the support with confocal microscopy; C. Bourgouin and the Center of Production and Infection of *Anopheles* (CEPIA-Institut Pasteur) for mosquito rearing; and G. Milon, G. Lauvau, and T. Graf for providing the *lys-gfp* mice.

This work was supported by funds from Pasteur Institute, the French National Research Agency (grant no. ANR-10-JCJC-1302-PlasmoPEP), the French Government's Investissement d'Avenir program, Laboratoire d'Excellence "Integrative Biology of Emerging Infectious Diseases" (grant no. ANR-10-LABX-62-IBEID), the European Community's Seventh Framework Programme (Evimalar, FP7/2007-2013, grant no. 242095), Natixis, and the Leukaemia and Lymphoma Research Funding (UK). J. Tavares was supported by a fellowship from the Fundação para Ciência e Tecnologia (SFRH/BPD/48340/2008) and P. Formaglio by a Ph.D. fellowship from the Direction Générale de l'Armement.

The authors have no competing financial interests.

Submitted: 26 May 2012
Accepted: 27 March 2013

REFERENCES

Amino, R., S. Thiberge, B. Martin, S. Celli, S. Shorte, F. Frischknecht, and R. Ménard. 2006. Quantitative imaging of *Plasmodium* transmission from mosquito to mammal. *Nat. Med.* 12:220–224. http://dx.doi.org/10.1038/nm1350

Amino, R., S. Thiberge, S. Blazquez, P. Baldacci, O. Renaud, S. Shorte, and R. Ménard. 2007. Imaging malaria sporozoites in the dermis of the mammalian host. *Nat. Protoc.* 2:1705–1712. http://dx.doi.org/10.1038/nprot.2007.120

Amino, R., D. Giovannini, S. Thiberge, P. Gueirard, B. Boisson, J.F. Dubremetz, M.C. Prévost, T. Ishino, M. Yuda, and R. Ménard. 2008. Host cell traversal is important for progression of the malaria parasite through the dermis to the liver. *Cell Host Microbe.* 3:88–96. http://dx.doi.org/10.1016/j.chom.2007.12.007

Baer, K., M. Roosevelt, A.B. Clarkson Jr., N. van Rooijen, T. Schnieder, and U. Frevert. 2007. Kupffer cells are obligatory for *Plasmodium yoelii* sporozoite infection of the liver. *Cell. Microbiol.* 9:397–412. http://dx.doi.org/10.1111/j.1462-5822.2006.00798.x

Barragan, A., F. Brossier, and L.D. Sibley. 2005. Transepithelial migration of *Toxoplasma gondii* involves an interaction of intercellular adhesion molecule 1 (ICAM-1) with the parasite adhesin MIC2. *Cell. Microbiol.* 7:561–568. http://dx.doi.org/10.1111/j.1462-5822.2005.00486.x

Bergmann-Leitner, E.S., P.M. Legler, T. Savranskaya, C.F. Ockenhouse, and E. Angov. 2011. Cellular and humoral immune effector mechanisms required for sterile protection against sporozoite challenge induced with the novel malaria vaccine candidate CelTOS. *Vaccine.* 29:5940–5949. http://dx.doi.org/10.1016/j.vaccine.2011.06.053

Downloaded from https://rupress.org/jem/article-pdf/210/5/905/639297/jem_20121130.pdf by guest on 28 May 2020

Bhanot, P., K. Schauer, I. Coppens, and V. Nussenzweig. 2005. A surface phospholipase is involved in the migration of *plasmodium* sporozoites through cells. *J. Biol. Chem.* 280:6752–6760. http://dx.doi.org/10.1074/jbc.M411465200

Carman, C.V., and T.A. Springer. 2004. A transmigratory cup in leukocyte diapedesis both through individual vascular endothelial cells and between them. *J. Cell Biol.* 167:377–388. http://dx.doi.org/10.1083/jcb.200404129

Carrolo, M., S. Giordano, L. Cabrita-Santos, S. Corso, A.M. Vigário, S. Silva, P. Leirião, D. Carapau, R. Armas-Portela, P.M. Comoglio, et al. 2003. Hepatocyte growth factor and its receptor are required for malaria infection. *Nat. Med.* 9:1363–1369. http://dx.doi.org/10.1038/nm947

Crompton, P.D., M.A. Kayala, B. Traore, K. Kayentao, A. Ongoiba, G.E. Weiss, D.M. Molina, C.R. Burk, M. Waisberg, A. Jasinskas, et al. 2010. A prospective analysis of the Ab response to *Plasmodium falciparum* before and after a malaria season by protein microarray. *Proc. Natl. Acad. Sci. USA.* 107:6958–6963. http://dx.doi.org/10.1073/pnas.1001323107

Ebrahimkhani, M.R., I. Mohar, and I.N. Crispe. 2011. Cross-presentation of antigen by diverse subsets of murine liver cells. *Hepatology.* 54:1379–1387. http://dx.doi.org/10.1002/hep.24508

Frevert, U., S. Engelmann, S. Zougbédé, J. Stange, B. Ng, K. Matuschewski, L. Liebes, and H. Yee. 2005. Intravital observation of *Plasmodium berghei* sporozoite infection of the liver. *PLoS Biol.* 3:e192. http://dx.doi.org/10.1371/journal.pbio.0030192

Frevert, U., I. Usynin, K. Baer, and C. Klotz. 2006. Nomadic or sessile: can Kupffer cells function as portals for malaria sporozoites to the liver? *Cell. Microbiol.* 8:1537–1546. http://dx.doi.org/10.1111/j.1462-5822.2006.00777.x

Helmy, K.Y., K.J. Katschke Jr., N.N. Gorgani, N.M. Kljavin, J.M. Elliott, L. Diehl, S.J. Scales, N. Ghilardi, and M. van Lookeren Campagne. 2006. CRIg: a macrophage complement receptor required for phagocytosis of circulating pathogens. *Cell.* 124:915–927. http://dx.doi.org/10.1016/j.cell.2005.12.039

Ishino, T., K. Yano, Y. Chinzei, and M. Yuda. 2004. Cell-passage activity is required for the malarial parasite to cross the liver sinusoidal cell layer. *PLoS Biol.* 2:E4. http://dx.doi.org/10.1371/journal.pbio.0020004

Ishino, T., Y. Chinzei, and M. Yuda. 2005. A *Plasmodium* sporozoite protein with a membrane attack complex domain is required for breaching the liver sinusoidal cell layer prior to hepatocyte infection. *Cell. Microbiol.* 7:199–208. http://dx.doi.org/10.1111/j.1462-5822.2004.00447.x

Ishino, T., Y. Orito, Y. Chinzei, and M. Yuda. 2006. A calcium-dependent protein kinase regulates *Plasmodium* ookinete access to the midgut epithelial cell. *Mol. Microbiol.* 59:1175–1184. http://dx.doi.org/10.1111/j.1365-2958.2005.05014.x

Kariu, T., T. Ishino, K. Yano, Y. Chinzei, and M. Yuda. 2006. CelTOS, a novel malarial protein that mediates transmission to mosquito and vertebrate hosts. *Mol. Microbiol.* 59:1369–1379. http://dx.doi.org/10.1111/j.1365-2958.2005.05024.x

Klotz, C., and U. Frevert. 2008. *Plasmodium yoelii* sporozoites modulate cytokine profile and induce apoptosis in murine Kupffer cells. *Int. J. Parasitol.* 38:1639–1650. http://dx.doi.org/10.1016/j.ijpara.2008.05.018

Klugewitz, K., F. Blumenthal-Barby, A. Schrage, P.A. Knolle, A. Hamann, and I.N. Crispe. 2002. Immunomodulatory effects of the liver: deletion of activated CD4+ effector cells and suppression of IFN-gamma-producing cells after intravenous protein immunization. *J. Immunol.* 169:2407–2413.

Meis, J.F., J.P. Verhave, P.H. Jap, and J.H. Meuwissen. 1983a. An ultrastructural study on the role of Kupffer cells in the process of infection by *Plasmodium berghei* sporozoites in rats. *Parasitology.* 86:231–242. http://dx.doi.org/10.1017/S003118200005040X

Meis, J.F., J.P. Verhave, P.H. Jap, R.E. Sinden, and J.H. Meuwissen. 1983b. Ultrastructural observations on the infection of rat liver by *Plasmodium berghei* sporozoites in vivo. *J. Protozool.* 30:361–366.

Moreira, C.K., T.J. Templeton, C. Lavazec, R.E. Hayward, C.V. Hobbs, H. Kroeze, C.J. Janse, A.P. Waters, P. Sinnis, and A. Coppi. 2008. The *Plasmodium* TRAP/MIC2 family member, TRAP-Like Protein (TLP), is involved in tissue traversal by sporozoites. *Cell. Microbiol.* 10:1505–1516. http://dx.doi.org/10.1111/j.1462-5822.2008.01143.x

Mota, M.M., and A. Rodriguez. 2004. Migration through host cells: the first steps of *Plasmodium* sporozoites in the mammalian host. *Cell. Microbiol.* 6:1113–1118. http://dx.doi.org/10.1111/j.1462-5822.2004.00460.x

Mota, M.M., G. Pradel, J.P. Vanderberg, J.C. Hafalla, U. Frevert, R.S. Nussenzweig, V. Nussenzweig, and A. Rodríguez. 2001. Migration of *Plasmodium* sporozoites through cells before infection. *Science.* 291:141–144. http://dx.doi.org/10.1126/science.291.5501.141

Mota, M.M., J.C. Hafalla, and A. Rodriguez. 2002. Migration through host cells activates *Plasmodium* sporozoites for infection. *Nat. Med.* 8:1318–1322. http://dx.doi.org/10.1038/nm785

Motta, P.M. 1984. The three-dimensional microanatomy of the liver. *Arch. Histol. Jpn.* 47:1–30. http://dx.doi.org/10.1679/aohc.47.1

Pradel, G., and U. Frevert. 2001. Malaria sporozoites actively enter and pass through rat Kupffer cells prior to hepatocyte invasion. *Hepatology.* 33:1154–1165. http://dx.doi.org/10.1053/jhep.2001.24237

Sinden, R.E., and J.E. Smith. 1982. The role of the Kupffer cell in the infection of rodents by sporozoites of *Plasmodium*: uptake of sporozoites by perfused liver and the establishment of infection in vivo. *Acta Trop.* 39:11–27.

Smedsrød, B., and H. Pertoft. 1985. Preparation of pure hepatocytes and reticuloendothelial cells in high yield from a single rat liver by means of Percoll centrifugation and selective adherence. *J. Leukoc. Biol.* 38:213–230.

Sturm, A., R. Amino, C. van de Sand, T. Regen, S. Retzlaff, A. Rennenberg, A. Krueger, J.M. Pollok, R. Menard, and V.T. Heussler. 2006. Manipulation of host hepatocytes by the malaria parasite for delivery into liver sinusoids. *Science.* 313:1287–1290. http://dx.doi.org/10.1126/science.1129720

Sturm, A., S. Graewe, B. Franke-Fayard, S. Retzlaff, S. Bolte, B. Roppenser, M. Aepfelbacher, C. Janse, and V. Heussler. 2009. Alteration of the parasite plasma membrane and the parasitophorous vacuole membrane during exo-erythrocytic development of malaria parasites. *Protist.* 160:51–63. http://dx.doi.org/10.1016/j.protis.2008.08.002

Talman, A.M., C. Lacroix, S.R. Marques, A.M. Blagborough, R. Carzaniga, R. Ménard, and R.E. Sinden. 2011. PbGEST mediates malaria transmission to both mosquito and vertebrate host. *Mol. Microbiol.* 82:462–474. http://dx.doi.org/10.1111/j.1365-2958.2011.07823.x

Tavares, J., P. Formaglio, A. Medvinsky, R. Ménard, and R. Amino. 2013. Imaging sporozoite cell traversal in the liver of mice. *Methods Mol. Biol.* 923:401–410. http://dx.doi.org/10.1007/978-1-62703-026-7_28

Thiberge, S., S. Blazquez, P. Baldacci, O. Renaud, S. Shorte, R. Ménard, and R. Amino. 2007. In vivo imaging of malaria parasites in the murine liver. *Nat. Protoc.* 2:1811–1818. http://dx.doi.org/10.1038/nprot.2007.257

Torgler, R., S.E. Bongfen, J.C. Romero, A. Tardivel, M. Thome, and G. Corradin. 2008. Sporozoite-mediated hepatocyte wounding limits *Plasmodium* parasite development via MyD88-mediated NF-kappa B activation and inducible NO synthase expression. *J. Immunol.* 180:3990–3999.

Van Rooijen, N., and A. Sanders. 1994. Liposome mediated depletion of macrophages: mechanism of action, preparation of liposomes and applications. *J. Immunol. Methods.* 174:83–93. http://dx.doi.org/10.1016/0022-1759(94)90012-4

Vanderberg, J.P., and U. Frevert. 2004. Intravital microscopy demonstrating antibody-mediated immobilisation of *Plasmodium berghei* sporozoites injected into skin by mosquitoes. *Int. J. Parasitol.* 34:991–996. http://dx.doi.org/10.1016/j.ijpara.2004.05.005

Vanderberg, J.P., S. Chew, and M.J. Stewart. 1990. *Plasmodium* sporozoite interactions with macrophages in vitro: a videomicroscopic analysis. *J. Protozool.* 37:528–536.

Vreden, S.G. 1994. The role of Kupffer cells in the clearance of malaria sporozoites from the circulation. *Parasitol. Today* (*Regul. Ed.*). 10:304–308. http://dx.doi.org/10.1016/0169-4758(94)90084-1

Warren, A., P. Bertolino, V. Benseler, R. Fraser, G.W. McCaughan, and D.G. Le Couteur. 2007. Marked changes of the hepatic sinusoid in a transgenic mouse model of acute immune-mediated hepatitis. *J. Hepatol.* 46:239–246. http://dx.doi.org/10.1016/j.jhep.2006.08.022

Wisse, E. 1974. Observations on the fine structure and peroxidase cytochemistry of normal rat liver Kupffer cells. *J. Ultrastruct. Res.* 46:393–426. http://dx.doi.org/10.1016/S0022-5320(74)90064-1

Xu, Y., L. Yuan, J. Mak, L. Pardanaud, M. Caunt, I. Kasman, B. Larrivée, R. Del Toro, S. Suchting, A. Medvinsky, et al. 2010. Neuropilin-2 mediates VEGF-C-induced lymphatic sprouting together with VEGFR3. *J. Cell Biol.* 188:115–130. http://dx.doi.org/10.1083/jcb.200903137

Yuda, M., and T. Ishino. 2004. Liver invasion by malarial parasites—how do malarial parasites break through the host barrier? *Cell. Microbiol.* 6:1119–1125. http://dx.doi.org/10.1111/j.1462-5822.2004.00474.x

Downloaded from https://rupress.org/jem/article-pdf/210/5/905/639297/jem_20121130.pdf by guest on 28 May 2020